CHARACTERIZING AN ALLEGED NEW PHASE OF TITANIUM DIOXIDE

Paul Atkinson

August 2007
Undergraduate Senior Capstone Project (Physics 492R)
Department of Physics and Astronomy
Brigham Young University

Due to a variety of potential scientific and industrial applications, a new phase of titanium dioxide (TiO_2) would be very exciting. I have investigated a powder sample, which based on preliminary chemical and structural analyses, appeared to be such a new phase. Through subsequent high-resolution x-ray powder diffraction, energy dispersive x-ray spectroscopy, and electron diffraction measurements, the sample has been identified as a dual-phase mixture of catalogued $Na_2Ti_3O_7$ and $Na_2Ti_6O_{13}$.

Research Advisor: Branton Campbell

INTRODUCTION

CRYSTAL STRUCTURES

A crystal phase is defined by its crystal structure, a parallelipiped-shaped unit cell containing the basic structural motif repeated throughout the crystal lattice. The unit cell is identified by lattice parameters—the lengths of the cell edges and the angles between them, labeled a, b, c, α, β and γ, as shown in Figure 1. Figure 2 illustrates the contents of the unit cell for a particular phase of titanium dioxide. Note that atoms are not necessarily located at the corners of a unit cell. A crystal's unit cell, lattice centering, and atomic positions can possess any one of 230 possible spacegroup symmetries and belong to any one of seven crystal systems which define all possible crystal systems.[1]

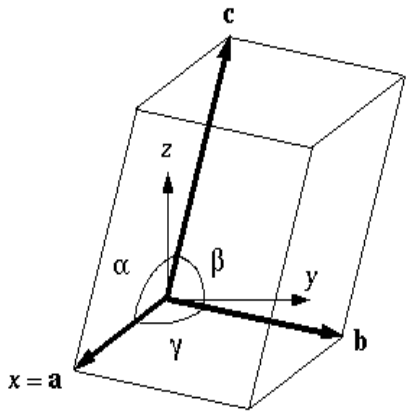

Figure 1. An arbitrary unit cell placed on a cartesian coordinate system.

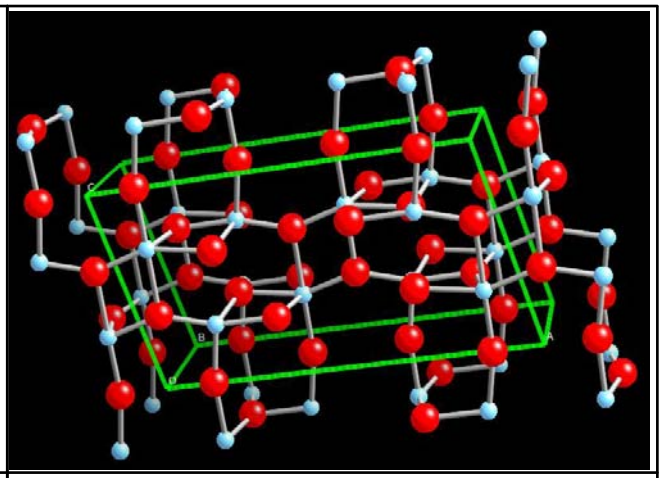

Figure 2. TiO_2(B) structure & unit cell. Lattice parameters: a=12.18 Å, b=3.74 Å, c=6.52 Å, α=γ=90.0°, β=107.1°. Space-group: C 2/m.

CRYSTALLOGRAPHY TECHNIQUES

Distances between a crystal's periodic atomic planes are termed *d*-spacings. While too minute to be measured with an optical microscope, they can be resolved using diffraction.

Bragg's Law, $n\lambda = 2d\sin\theta$, relates the wavelength of a probe beam, the measured angles of constructive interference and a crystal's *d*-spacings.

Figure 3 shows an electron diffraction pattern produced in a transmission electron microscope (TEM). The reciprocal of the distance of each diffraction spot from the bright, central beam spot reveals one of the crystal's *d*-spacings. The angles between intersecting rows of spots correlate to the angles between intersecting planes of atoms. By combining angular and length data from multiple electron diffraction patterns a crystal structure can be solved.

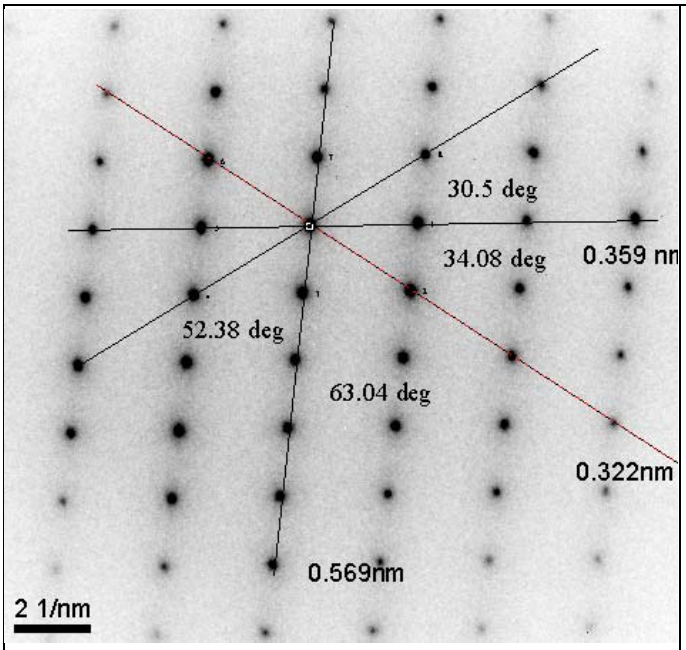

Figure 3. Sample electron diffraction pattern. Rows of diffraction peaks correlate to inter-planar *d*-spacings. Angles between these rows likewise correlate to angles between planes of atoms. Lengths in electron diffraction patterns are derived from reciprocal space (note how larger spacings in the pattern are assigned shorter lengths.

Electron diffraction can examine a single nano-crystal because of the short wavelengths of electrons ($\lambda = 0.0025$ *nm* at 200 keV)—ideal when only a powder sample is available. However, because of calibration difficulties, measured distances in electron diffraction patterns are not highly accurate. Unless checked against a standard at the time of acquisition, only ratios of lengths can be trusted with confidence. Another drawback stems from the TEM sample holder's limited range of tilt, which prohibits an extensive three-dimensional analysis of reciprocal space. Consequently, patterns from multiple grains with unrelated orientations must

be collected and correlated. The difficulty of the task is then multiplied with the presence of more than one distinct phase in a sample.

In powder X-ray diffraction (PXD) experiments, many small, arbitrarily-oriented crystals create a single pattern from which many of a crystal's *d*-spacings can be derived. A key advantage of PXD is the accuracy of its *d*-spacing measurements. But because PXD patterns are averages over random single-crystal orientations, one cannot directly determine the physical angles between distinct peaks. Powder indexing procedures, however, can still be used to obtain the angles in many cases. Experimental PXD data are often analyzed by comparison with computer databases of experimental and calculated patterns, as in Figure 4.[2]

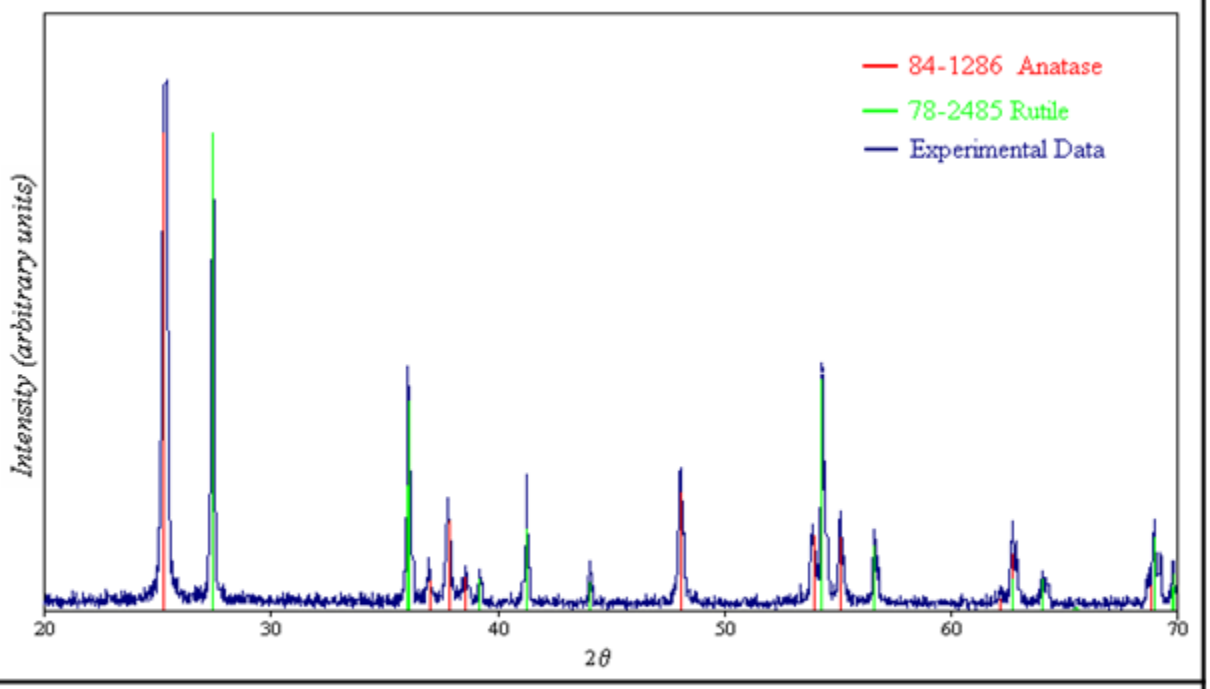

Figure 4. Sample XPD pattern with matching catalogued peaks.

SYNTHESIS MOTIVATION AND EARLY CHARACTERIZATION EFFORTS

North American factories produced 1,728 thousand metric tons of TiO_2 in 2003. A quantitative breakdown of TiO_2 uses for industrial applications is shown in Figure 5.[3] TiO_2

properties allow it to function as a whitening pigment, UV reflective coating, dielectric mirror coating, sanitizing and deodorizing coating, opacity increaser, and thickening agent. Three common phases of TiO_2 exist, namely anatase, rutile, and brookite. In 1980, a monoclinic form was synthesized and named TiO_2-B because it shares the *b*-length lattice parameter of anatase. Anatase, TiO_2-B, and various doped-derivates have outstanding photocatlatyic properties that are currently under investigation as part of efforts to efficiently harness solar energy.[4-6]

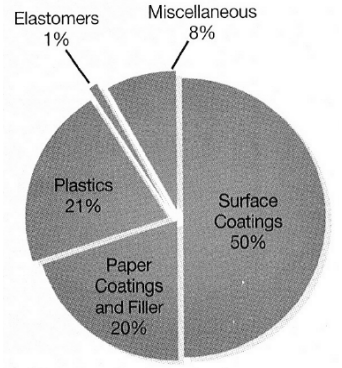

Figure 5. TiO_2 applications

A powder sample prepared by Dr. Guangshe Li in the group of Brian Woodfield and Julie Boerio-Goates (BYU Chemistry), when subjected to bulk-elemental analysis, initially appeared to contain only titanium and oxygen. A new phase of TiO_2 was suspected—a potentially significant discovery. When PXD patterns failed to match any one entry in the PDF database, synchrotron x-ray powder diffraction data was collected using the high-intensity X7A beamline at Brookhaven National Laboratory (BNL). Multiple algorithms failed at indexing the resulting PXD patterns despite the quality of the data. This failure suggested either a modulated structure or a mixed-phase sample.

METHODS

To better determine the sample's composition, we used the Energy-Dispersive X-ray Spectroscopy (EDX) capabilities of BYU's Tecnai TF-20 (200 keV) electron microscope. EDX involves the electron-bombardment of a sample and subsequent measurement of emitted x-ray energies. Composition ratios were determined with the Digital Micrograph[7] software by comparing x-ray energies with the unique spectral-line fingerprints of each element. We did not use a known standard to calibrate the software's absorption ratios, and thus can only rely on the Digital Micrograph calibrations for approximate stoichiometric ratios. Five grains of the sample were examined by EDX. Area scan tests were applied as shown in Figure 6.

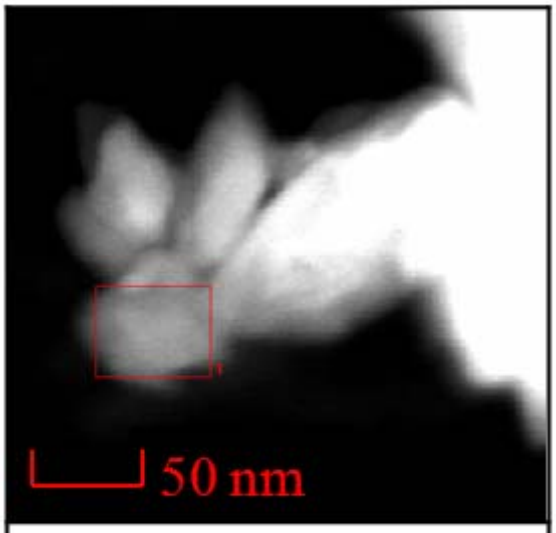

Figure 6. EDX area (red box) scan in TEM.

JADE[8] is an advanced powder diffraction processing software suite. We used it to analyze the synchrotron powder diffraction data, to compare powder patterns from the PDF database, and to simulate and compare candidate unit cells.

BYU microscopist Jeff Farrer and BYU Summer 2006 REU student Jose Zalles collected 98 electron diffraction patterns from 23 different grains using the Tecnai TF-30 TEM. Many of

these patterns proved helpful in the present analysis. Microscope slides of the sample were prepared by dusting a few milligrams of the sample onto a carbon wafer and then blowing off most of the particles with a can of air, so that some particles remained isolated across the wafer slide. Major lengths and angles in the captured diffraction pattern images were measured using the Digital Micrograph software. So as to know the window of error in these measurements, I zoomed into the pixel level and averaged *d*-spacing measurements that I knew to be slightly larger and slightly smaller than the actual lengths and angles observed.

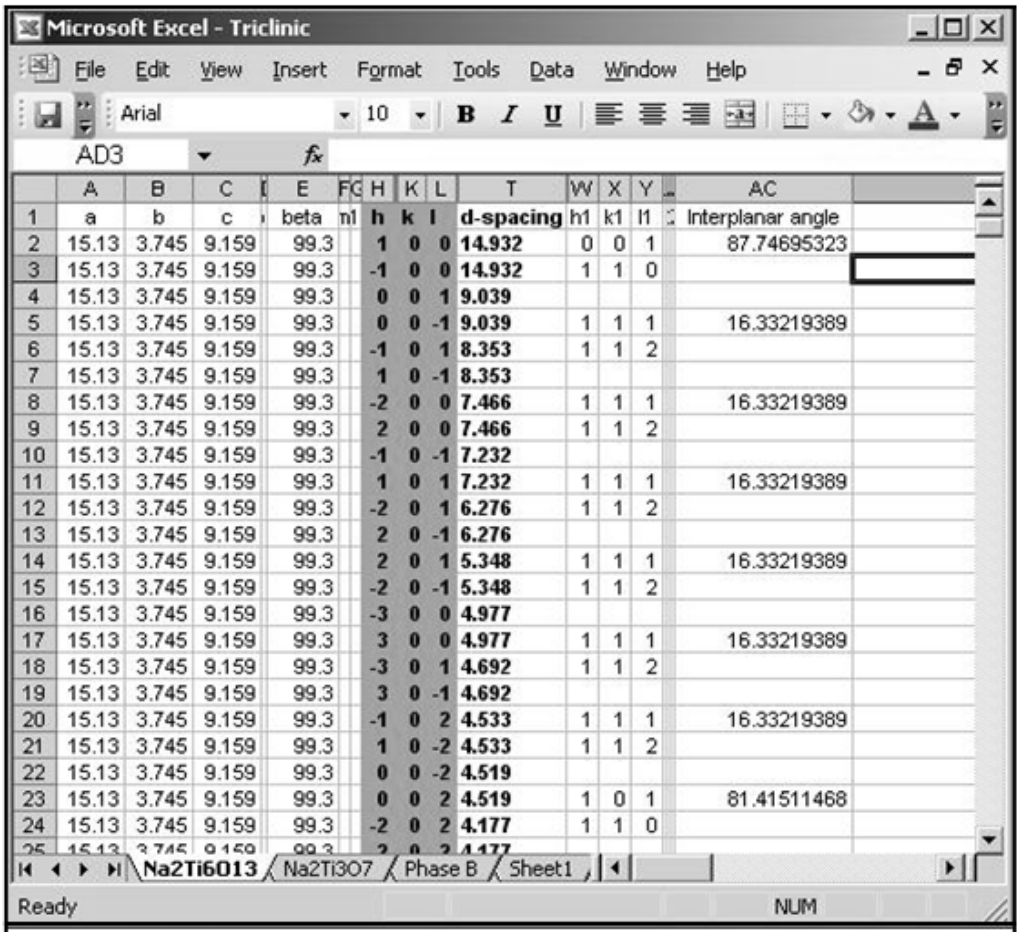

	A	B	C	E	H	K	L	T	W	X	Y	AC
1	a	b	c	beta	h	k	l	d-spacing	h1	k1	l1	Interplanar angle
2	15.13	3.745	9.159	99.3	1	0	0	14.932	0	0	1	87.74695323
3	15.13	3.745	9.159	99.3	-1	0	0	14.932	1	1	0	
4	15.13	3.745	9.159	99.3	0	0	1	9.039				
5	15.13	3.745	9.159	99.3	0	0	-1	9.039	1	1	1	16.33219389
6	15.13	3.745	9.159	99.3	-1	0	1	8.353	1	1	2	
7	15.13	3.745	9.159	99.3	1	0	-1	8.353				
8	15.13	3.745	9.159	99.3	-2	0	0	7.466	1	1	1	16.33219389
9	15.13	3.745	9.159	99.3	2	0	0	7.466	1	1	2	
10	15.13	3.745	9.159	99.3	-1	0	-1	7.232				
11	15.13	3.745	9.159	99.3	1	0	1	7.232	1	1	1	16.33219389
12	15.13	3.745	9.159	99.3	-2	0	1	6.276	1	1	2	
13	15.13	3.745	9.159	99.3	2	0	-1	6.276				
14	15.13	3.745	9.159	99.3	2	0	1	5.348	1	1	1	16.33219389
15	15.13	3.745	9.159	99.3	-2	0	-1	5.348	1	1	2	
16	15.13	3.745	9.159	99.3	-3	0	0	4.977				
17	15.13	3.745	9.159	99.3	3	0	0	4.977	1	1	1	16.33219389
18	15.13	3.745	9.159	99.3	-3	0	1	4.692	1	1	2	
19	15.13	3.745	9.159	99.3	3	0	-1	4.692				
20	15.13	3.745	9.159	99.3	-1	0	2	4.533	1	1	1	16.33219389
21	15.13	3.745	9.159	99.3	1	0	-2	4.533	1	1	2	
22	15.13	3.745	9.159	99.3	0	0	-2	4.519				
23	15.13	3.745	9.159	99.3	0	0	2	4.519	1	0	1	81.41511468
24	15.13	3.745	9.159	99.3	-2	0	2	4.177	1	1	0	
25	15.13	3.745	9.159	99.3	2	0	2	4.177				

Figure 7. Screenshot from Excel sorting file.

I created a model of the crystal with the CrystalMaker[9] software using lattice and atomic-position data supplied by primary literature sources for catalogued phases.[10-11] I used the SingleCrystal[12] software to simulate electron diffraction patterns of the models created in

CrystalMaker. Using a Microsoft Excel spreadsheet, I then calculated *d*-spacings and inter-planar angles for specific atomic planes from unit cell parameters (see Figure 7). Using the spreadsheet's sorting capabilities, I sought to match experimentally-measured angles and length ratios with calculated angles and length ratios. When feasible matches appeared, I simulated the pattern in SingleCrystal and compared it to the experimental pattern.

RESULTS AND DISCUSSION

COMPOSITIONAL ANALYSIS

EDX compositional analysis showed the sample to have an average approximate stochiometry of $Na_{0.51}TiO_{1.82}$. Trace amounts of copper and silicon were also detected. The result of one EDX scan is shown in Figure 8. The sodium presence was unexpected and eliminated the possibility of having a new phase of TiO_2. Sodium was used during the synthesis process and evidently was incorporated. Copper and silicon were minor contaminants.

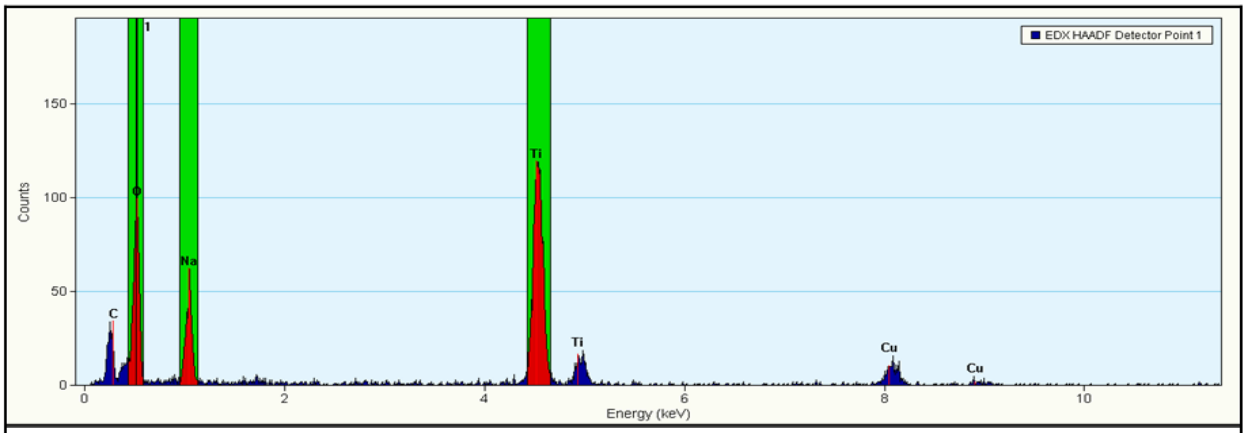

Figure 8. Results of an EDX scan. Characteristic energy peaks reveal atomic composition. Shaded regions indicate which peaks were selected for relative mass analysis. The carbon peak is from the wafer slide used to hold the sample.

POWDER DIFFRACTION

JADE's algorithms were unable to extract a feasible unit cell from the synchrotron powder diffraction data. It also failed to match the synchrotron powder diffraction data to any

patterns in its database. Searching the PDF database for compounds containing only sodium and titanium and oxygen returned 56 compounds (including multiple duplicates), ranging from $NaTi_8O_{13}$ to $Na_4Ti_{0.3}O_2$. Using JADE to compare these compounds' powder patterns with the experimental pattern yielded two outstanding partial matches: $Na_2Ti_3O_7$ and $Na_2Ti_6O_{13}$, shown in Figures 9 and 10.

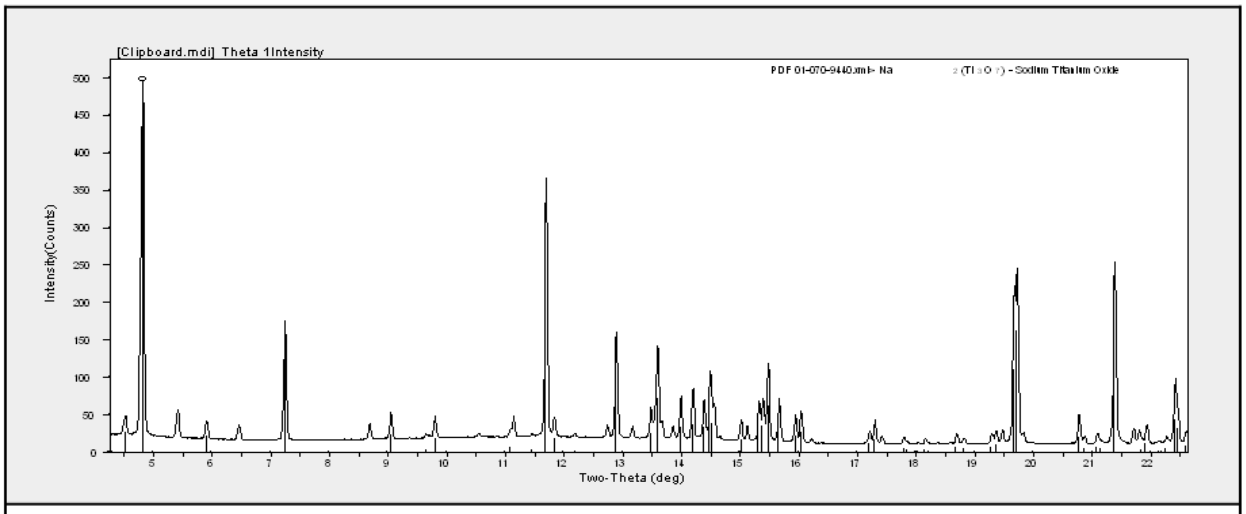

Figure 9. Overlay of BNL pattern with catalogued $Na_2Ti_3O_7$ peaks.

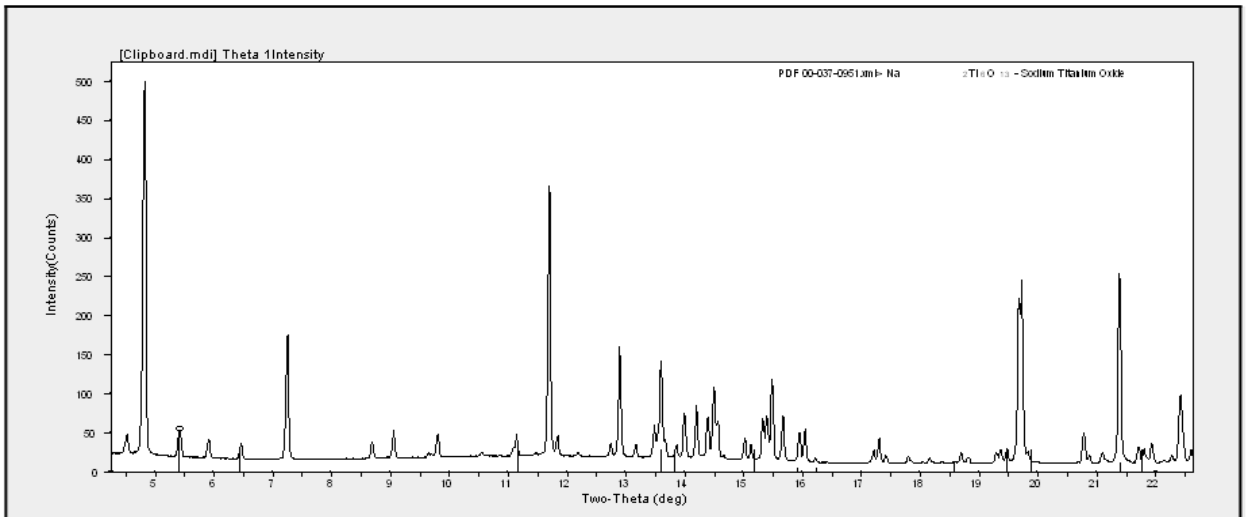

Figure 10. Overlay of BNL pattern with catalogued $Na_2Ti_6O_{13}$ peaks.

The accuracy with which the peaks of the catalogued $Na_2Ti_3O_7$ and $Na_2Ti_6O_{13}$ compounds matched the experimental data is convincing evidence that both of these compounds are in the sample. This is further emphasized by considering Figure 11, which overlays the

experimental data with the catalogued peaks of both $Na_2Ti_3O_7$ and $Na_2Ti_6O_{13}$. 90% of the major peaks in the sample's pattern are matched by one of the peaks from the two known compounds, and the intensities exhibit roughly the expected trends. The fact that some of the observed peaks don't match either phase suggests the presence of additional minor phases that we are unable to identify. $Na_2Ti_3O_7$ has parameters a=9.133(2) Å, b=3.806(2) Å, c=8.566(2) Å and β=101.57(3) and $Na_2Ti_6O_{13}$ has parameters a=15.131(2) Å, b=3.745(2) Å, c=9.159(2) Å and β=99.3(5).[10,11]

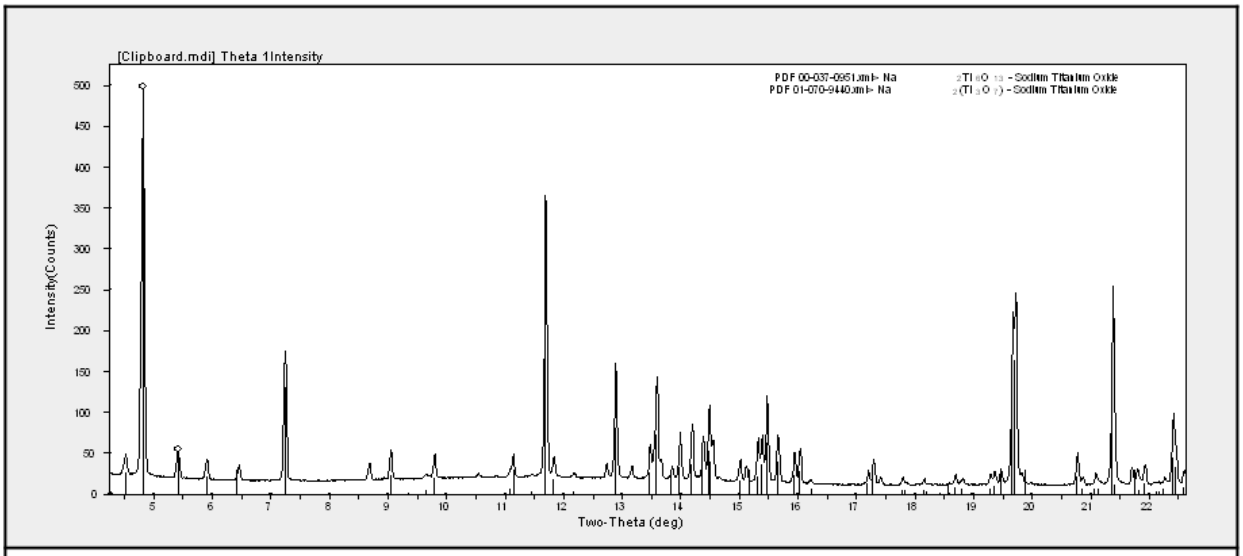

Figure 11. Combined overlay of BNL pattern with catalogued $Na_2Ti_3O_7$ and $Na_2Ti_6O_{13}$ peaks.

ELECTRON DIFFRACTION

The first set of electron diffraction patterns we acquired suggested a potential monoclinic unit cell. A second collection revealed unexpected d-spacings which failed to correlate with our originally proposed unit cell. As we collected additional data, a large distribution of inter-planar spacings became apparent. A single, feasibly-sized unit cell likely could not account for the variety of major *d*-spacings extracted from the diffraction patterns, suggesting that there were in fact multiple phases.

Eventually, matching PXD patterns confirmed the presence of at least two constituents, $Na_2Ti_3O_7$ and $Na_2Ti_6O_{13}$. Even with the known parameters of these two phases, confidently

identifying the various electron diffraction patterns remained elusive. Too many experimentally extracted *d*-spacings did not match the calculated values derived from the two known phases. This discrepancy was resolved by comparing the *ratios* of the two most prominent *d*-spacings in experimental and simulated electron diffraction patterns. While calibration can introduce a factor of error in all measured lengths of an electron diffraction pattern, dividing these lengths to obtain a ratio cancels out these inaccuracies. Using ratios, Figures 12-14 compare observed and simulated diffraction patterns based on *d*-spacing ratios. Evaluating the patterns, we see that the *d*-spacing ratios and angles match reasonably well, while differences in spot intensities indicate differences in the details of the crystal structure. This is the case in original publications as well.[10-11]

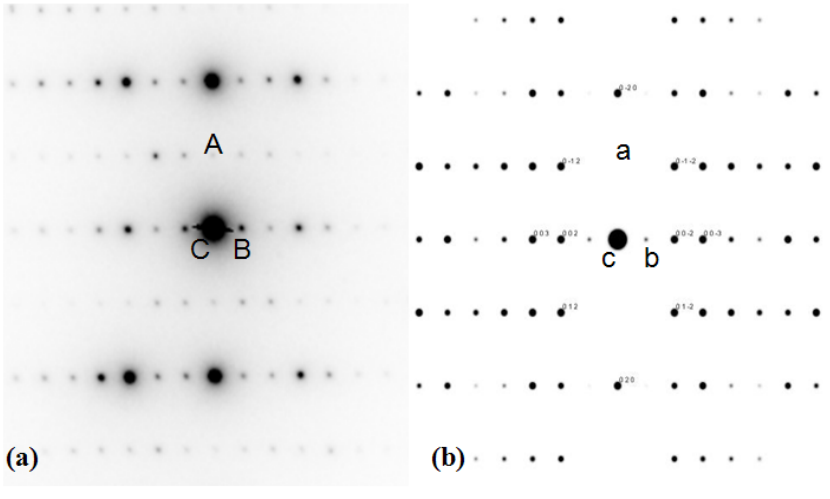

Figure 12 (a) Observed pattern. **(b)** Simulated pattern of $Na_2Ti_3O_7$ from the [1,0,0] zone. Observed major lengths ratio (AC/BC): 2.36 ± .057. Simulated major lengths ratio (ac/bc): 2.353. Observed major angle (ACB): 90.34° ± .58. Simulated major angle (acb): 90.00°.

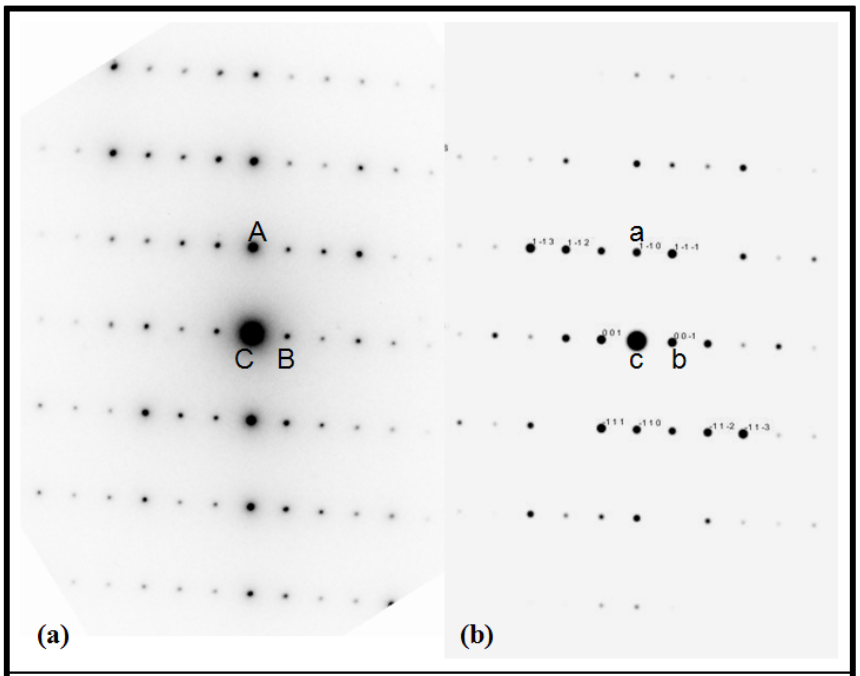

Figure 13 (a) Observed pattern. **(b)** Simulated pattern of $Na_2Ti_3O_7$ from the [1,-1,1] zone. Observed major lengths ratio (AC/BC): 1.99 ± .046. Simulated major lengths ratio (ac/bc): 1.976. Observed major angle (ACB): 73.85° ± .51. Simulated major angle (acb): 74.15°.

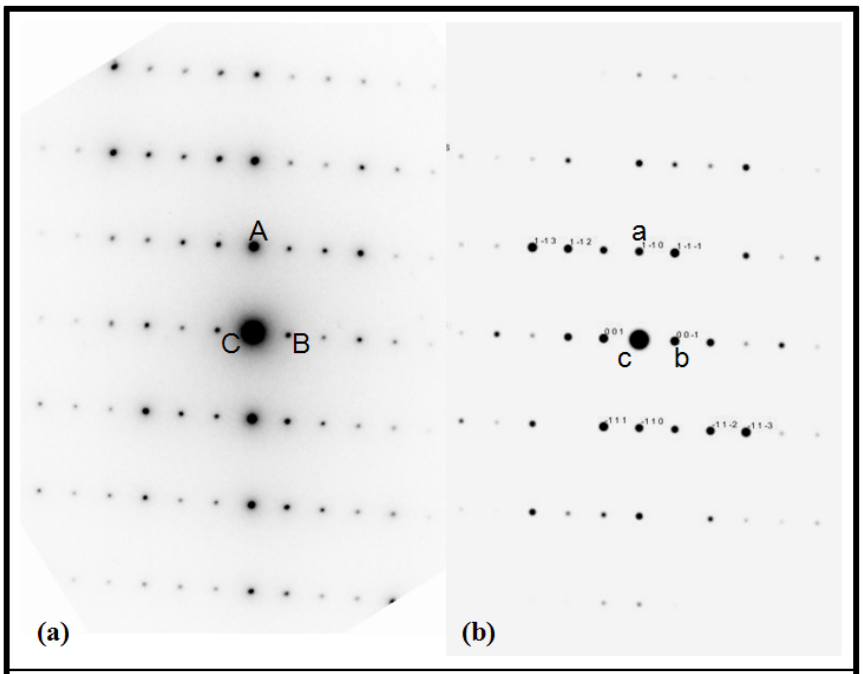

Figure 14 (a) Observed pattern. **(b)** Simulated pattern of $Na_2Ti_6O_{13}$ from the [1,1,0] zone. Observed major lengths ratio (AC/BC): 2.43 ± .028. Simulated major lengths ratio(ac/bc): 2.448. Observed major angle (ACB): 86.80° ± .37. Simulated major angle (acb): 87.75°.

CONCLUSIONS

The alleged new phase of TiO_2 was revealed by EDX analysis to be a sodium titanate. Initial efforts to characterize the unit cell parameters from PXD failed, not because the sample has an irregular unit cell, but because it is multi-phased combination of primarily $Na_2Ti_3O_7$ and $Na_2Ti_6O_{13}$. Matching PXD and electron diffraction patterns verified the presence of these phases. Both are documented in the literature, but their combination produced a unique and seemingly complex powder pattern. Awareness of this sodium titanate family of compounds will be valuable in future TiO_2 synthesis and characterization efforts.

ACKNOWLEDGEMENTS

I first acknowledge my advisor Branton Campbell for generously given direction, expertise, encouragement, and patience in all aspects of the project. Thanks also to Jeff Farrer and Jose Zalles for hours spent collecting electron diffraction patterns, Steven Herron for his efforts with single crystals and JADE, and Richard VanFleet for his help in interpreting electron diffraction patterns.

REFERENCES

1 Spacegroup details are fundamental to crystallography but beyond the scope of this paper. See, for example, The Basics of Crystallography and Diffraction, 2nd Edition, C. Hammond, New York: Oxford University Press, 2001.
2 Anatase and rutile XRD phase identification analysis, www.hkbu.edu.hk/~csar/phase_identification.html.
3 M. Kirschner, Chemical Market Reporter **263**, 31 (June 2, 2003).
4 J. Jun, M. Dhayal, J. H. Shin, J.C. Kim, and N. Getoff. Radiation Physics and Chemistry **75**, 583-589 (2006).
5 M. Ni, M. K. H. Leung, D. Y. C. Leung, and K. Sumathy. Renewable and Sustainable Energy Reviews **11**, 401-425 (2007).
6 H. L. Kuo, C. Y. Kuo, C. H. Liu, J. H. Chao and C. H. Lin, Catalysis Letters **113**, 7-12 (2007).
7 Digital Micrograph software, version 3.6.5. Gatan Incorporated. www.gatan.com.
8 JADE software, version 8.0. Materials Data Incorporated. www.materialsdata.com.
9 CrystalMaker software, version 1.4.2. CrystalMaker Software Limited. www.crystalmaker.com.
10 S. Andersson and A. D. Wadsley, Acta Cryst. **14**, 1245-1249 (1961).
11 S. Andersson and A.D. Wadsley, Acta Cryst. **15**, 194-201 (1962).
12 SingleCrystal software, version 1.0.2. CrystalMaker Software Limited. www.crystalmaker.com.